# HDVIP HgCdTe and Silicon Detectors and FPAs for Remote Sensing Applications

**A.I. D'Souza, M.G. Stapelbroek, E. Atkins, H. Hogue, J. Reekstin**
*DRS Sensors& Targeting Systems, 10600 Valley View St., Cypress, CA 90630*

**H-D Shih, M. Skokan, M. Kinch, J. Robinson**
*DRS Infrared Technologies, Dallas, TX*

## 1. ABSTRACT

Photon detectors and focal plane arrays (FPAs) are fabricated at DRS from HgCdTe and silicon in many varieties. Remote sensing applications, however, may need to operate under both high and low background conditions. HgCdTe HDVIP FPAs have been measured under a variety of flux conditions and at several operating temperatures. In addition, DRS manufactures silicon detectors and FPAs that cover the spectral range from visible to the very-long-wavelength infrared (VLWIR). Large-format, VLWIR FPAs based on doped-silicon Blocked-Impurity-Band (BIB) detectors have been developed. FPAs with Si:As BIB arrays have been made in a variety of pixel formats (up to $1024^2$) and have been optimized for low, moderate, and high infrared backgrounds.

DRS uses LPE-grown SWIR, MWIR and LWIR HgCdTe material to fabricate High-Density Vertically Integrated Photodiode (HDVIP) architecture detectors. 2.5 μm, 5.3 μm and 10.5 μm cutoff detectors have been fabricated into linear arrays as technology demonstrations targeting remote sensing programs. This paper presents 320 x 6 array configuration technology demonstrations' performance of HDVIP HgCdTe detectors. Within the arrays, the detector size is 40 μm x 50 μm. The MWIR detector array has a mean quantum efficiency of 89.2 % with a standard deviation to mean ratio, $\sigma/\mu$ = 1.51 %. The integration time for the focal plane array (FPA) measurements is 1.76 ms with a frame rate of 557.7 Hz. NEI $\sigma/\mu$ = 3.0 % was measured with 100 % operability when running the array in the best detector select mode.

Arsenic-doped silicon (Si:As) BIB detector arrays with photon response out to about 28 μm, and Antimony-doped silicon (Si:Sb) BIB arrays having response to wavelengths > 40 μm have been demonstrated. Large-format (1024 x 1024) VLWIR FPAs based on doped-silicon BIB detectors has been developed and are in fabrication. These FPAs comprise an array of BIB detectors interfaced via indium column interconnects to a matching read-out integrated circuit (ROIC). 256 x256 Arsenic-doped silicon (Si:As) BIB detector arrays with photon response out to about 28 μm have been measured with a 99.995 % operability and a response standard deviation to mean ratio of 1.58 %. FPAs with Si:As BIB arrays have been made in a variety of pixel formats (to $1024^2$) have been optimized for low, moderate, and high infrared backgrounds.

DRS has developed techniques that allow precision photolithographic backside processing on thinned silicon detector wafers . This capability has been used to monolithically fabricate novel, high performance optical elements such as wire grid polarizers and diffractive lenslets on Si:As BIB arrays. This technique has been used to manufacture and demonstrate advanced sensors including real-time polarimetric imaging arrays capable of fully characterizing the linear polarization state of scene elements. The capability has been used extensively for targeting and image enhancement with LWIR sensors. Non-monolithic prototypes for the visible and LWIR wavebands have been assembled using commercial CCD imaging chips and LWIR HgCdTe arrays. Performance of these visible polarimetric imaging devices has been constrained by several factors including their non-monolithic construction. DRS can apply the process techniques already demonstrated with LWIR FPAs to Si *p-i-n* arrays being developed and enable high performance visible wavelength polarimetric staring arrays suitable for potential SSA needs.

## 2. INTRODUCTION

SWIR, MWIR and LWIR HgCdTe linear arrays with 100 % operability were required for remote sensing applications. To increase yield, the ROIC is designed to have a 320 x 6 format with one of the ROIC features being that the best detector in every row of six detectors is selected to be part of the 320 x 1 linear array. Although technology demonstrations encompassed $\lambda_c$ = 2.5 μm, 5.3 μm and 10.5 μm detector arrays, this paper focuses on the

$\lambda_c$ = 5.3 μm array. However, data is presented on LWIR $\lambda_c$ = 10.5 μm single detector noise as a function of frequency. Response and noise measurements made on the 320 x 6 arrays demonstrated the capability of the HDVIP architecture to meet nominal remote sensing NEI flow down requirements with margin.

When originally developed, BIB detector technology was aimed at low flux applications, particularly space-based applications such as astronomy and surveillance with cooled optical systems. Higher flux applications have required significant modifications to the detector materials and architecture to address signal linearity, array spatial uniformity, and excess low-frequency noise (ELFN). The most mature variety of BIB detector is based on arsenic-doped silicon (Si:As), although BIB detectors and focal plane arrays (FPAs) using several other dopants have been demonstrated. Read-out integrated circuits (ROICs) and matching detector arrays have been designed, fabricated, and hybridized to demonstrate hybrid arrays for low, moderate, or high flux ranges in formats as large as 1024x1024.

This same architecture and Si processing capability has been used to fabricate visible wavelength *p*-*i*-*n* diode arrays. These arrays can utilize the same ROIC inventories that have been developed over the past decade for the BIB arrays. This allows us to leverage the large investment in ROIC design and fabrication for use with visible wavelength FPAs.

## 3. HDVIP ARCHITECTURE

HDVIP HgCdTe detector is a front-side illuminated, planar, *n*-on-*p*, structure [1]. Strengths of the vertically integrated photodiode approach include high D*, near theoretical MTF, excellent quantum efficiency, stability over extended bakes at 100°C, immunity to degradation by thermal cycling, and producibility. The detector is fabricated on a thinned *p*-type HgCdTe LPE layer that is doped extrinsically by impurities and intrinsically by metal site vacancies. Passivation is accomplished using an evaporated CdTe layer [1]. The connection of the *n*-side of the junction to the underlying ROIC is made through an electron cyclotron resonance (ECR)-etched vertical via in the unit cell. The etching process produces Hg interstitials that annihilate vacancies and sweep fast diffusing impurities away from the via, resulting in a radial $n^-$ region doped with indium and a p-type region doped with Cu. A Hg vacancy concentration of $V_{Hg}$ ~$10^{16}$ $cm^{-3}$ is required to stabilize the Cu. A deposited metal film connects the diode via sidewalls to the landing pad on the ROIC or fanout chip. Details of the detector architecture have been described previously [2].

## 4. HgCdTe 320 x 6 FPA CONFIGURATION and DATA

SWIR ($\lambda_c$ = 2.5 μm), MWIR (($\lambda_c$ = 5.3 μm) and LWIR (($\lambda_c$ = 10.5 μm) HgCdTe material is grown by liquid phase epitaxy (LPE) prior to High-Density Vertically Integrated Photodiode (HDVIP) architecture detector fabrication. Presented here are MWIR (SWIR and LWIR data references[3,4]) data from 320 x 6 array configuration technology demonstrations' performance of HDVIP HgCdTe detectors. The MWIR detector array has a mean quantum efficiency of 89.2 % with a standard deviation to mean ratio, $\sigma/\mu$ = 1.51 %. The integration time for the focal plane array (FPA) measurements is 1.76 ms with a frame rate of 557.7 Hz. The responses for all 320 x 6 detectors in the array are shown in Figure 1. The $\cos^4$ (illumination) correction has not been applied to the response data. Only nine detectors have responses not in line with the rest of the detectors in the array. If the array is to be used as a single 320 x 1 linear array, the best detector from each row of six detectors can be selected by the ROIC (best detector select or BDS mode). This BDS mode allows the selection of a single detector from each row of six, providing a 100% operable highest performance linear 320 x 1 array, albeit one consisting of staggered detectors [4]. Operating in the BDS mode, noise as a function of flux was measured and is displayed in Figure 2. At a nominal 9.45 x $10^{12}$ $ph/cm^2/s$ flux, the noise is near photon shot noise dominated and is equal to the modeled 612 μV total noise which includes detector dark shot and 1/f, photon shot and 1/f, ROIC and test station noise. NEI is plotted in Figure 3 for the same 320 x 1 detectors shown in Figure 2. MWIR NEI data demonstrates high uniformity with a tight $\sigma/\mu$ = 3.0 %. Using the BDS mode a 100% operability linear array is obtained.

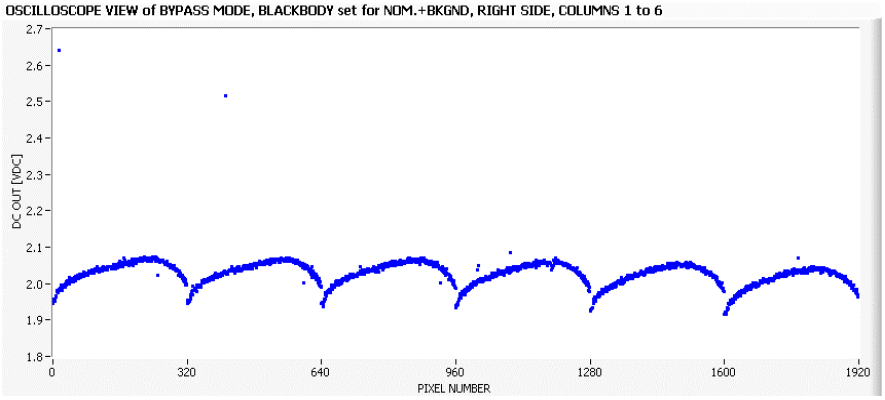


Figure 1. Response data for all the 320 x 6 detectors in the $\lambda_c \approx 5.3$ µm cut-off array

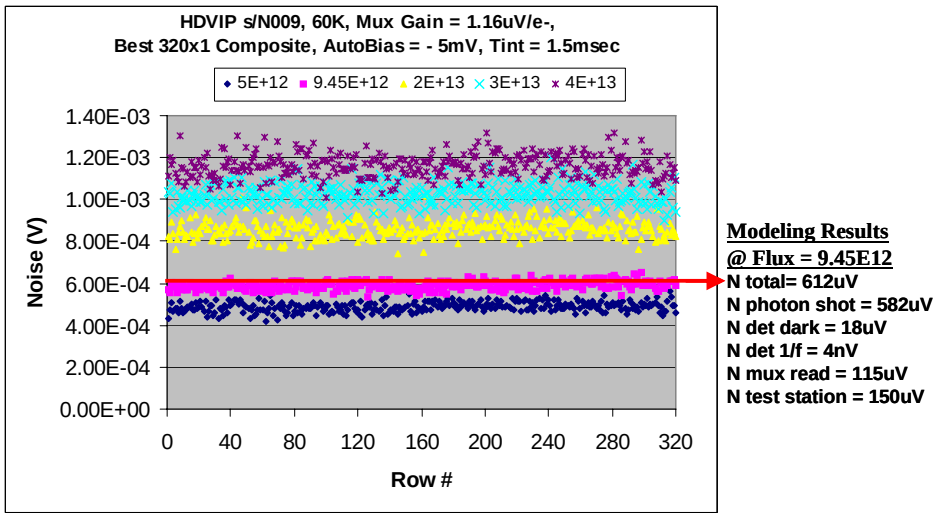


Figure 2. Noise Measurements Agree with Model

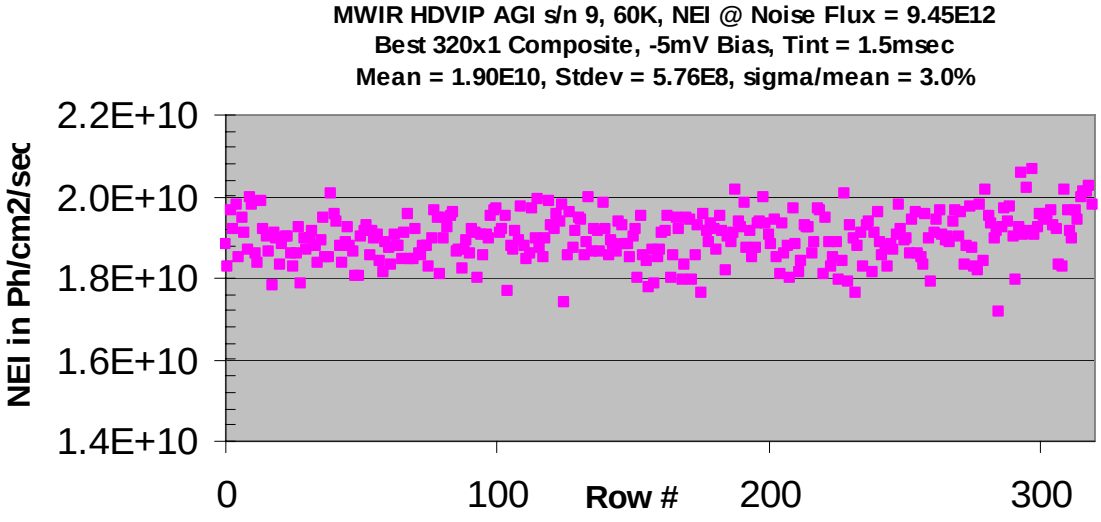


Figure 3. NEI for best detector select mode 320 rows

## 5. Si BLOCKED-IMPURITY-BAND (BIB) DETECTOR ARCHITECTURE

Si:As hybrid focal plane arrays (FPAs) are optimized for either high, moderate, or low infrared background applications ($10^{14}$, $10^{12}$, $<10^{10}$ photons/cm2/s, respectively) in formats up to 256 x 256. Additionally, several low-background 1024 x 1024 Si:As FPAs have been demonstrated. BIB detectors offer high quantum efficiency over a very broad range of infrared wavelengths combined with excellent response uniformity ($\sigma/\mu < 0.02$), operability (typically > 0.995) and stability along with an inherent tolerance for nuclear radiation. Antimony-doped silicon (Si:Sb) BIB detector arrays with spectral response out to 40 microns have been developed and two 128x128 Si:Sb FPAs will be flown on the SIRTF astronomy satellite's Infrared Spectrograph (IRS) instrument. Other material systems investigated for BIB detector application include phosphorus-doped silicon (Si:P), gallium-doped silicon (Si:Ga), gallium-doped germanium (Ge:Ga), and boron-doped germanium (Ge:B).

A passive, exoatmospheric seeker, benefits by using all the available photons thereby increasing acquisition range and improving temperature-based discrimination capabilities. Most of the photons emitted by a gray body near or below room temperature are at wavelengths longer than 12 μm. Further, the combined requirements of lightweight, low cost, rapid cooldown, and low maintenance preclude the use of a cryogenically cooled optical system. A warm optical system, in turn, requires the focal plane array to handle a high infrared background. High-flux Si:As FPAs which utilize the broad LWIR spectrum of targets of interest for exoatmospheric seekers have been optimized for such applications.

BIB detector physics, models, and performance have been published previously [5, 6], only salient features are summarized here. BIB detectors effectively use the hopp-i-ng conductivity associated with "impurity banding" in relatively heavily doped semiconductors (specifically single-crystalline Si:As for this discussion). In particular, a BIB detector comprises two thin epitaxial layers placed between planar electrical contacts; a relatively heavily doped infrared active layer and an undoped or lightly doped blocking layer. Figure 4 illustrates the structure of a BIB detector constructed to allow back-illumination through a transparent silicon substrate. All active detector structures are fabricated on the front side of the undoped single-crystal substrate wafer.

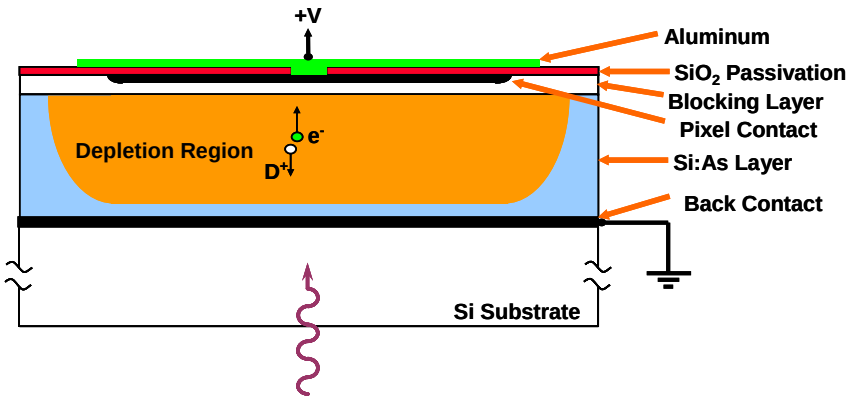


Figure 4. Layer structure for a Si:As BIB detector

Because of the presence of the blocking layer, BIB detectors do not follow the usual photoconductor model. The behavior of BIB detectors is closer to that of a reverse-biased photodiode except that photoexcitation of electrons occurs from the donor impurity band to the conduction band. The gap between the impurity band and the conduction band is narrow; therefore, the response of a Si:As BIB detector extends to the VLWIR region of the spectrum. Thermal excitation of electrons across the narrow bandgap leads to dark current and the detectors must be operated at temperatures sufficiently low (T < 13 K) to limit the dark current.

## 6. BIB DATA

Figure 5 illustrates dark current versus temperature for BIB detector material optimized for low background applications. Dark currents < 1e-/sec/pixel are achieved at temperatures above 6K for standard LWIR arrays.

Cooling below 6 K further reduces the dark current. An Arrhenius plot of this data shows the expected BIB thermal activation energy of 27 meV. For BIB arrays optimized for high background applications the dark current values will be approximately an order of magnitude higher and the activation energy a bit lower (~ 24 meV). Figure 6 is the quantum yield versus wavelength plot of a Si:As BIB detector showing response out to ~ 28 μm although the detector has been AR-coated for peak response at 11.5 μm [7]. The dip in the quantum yield at ~ 9 mm is due to asymmetric stretching of the two Si-O bonds. Shown in Figure 7 is the response data from a 256 x 256 Si:As BIB focal plane array (FPA). Only 3 out of 65536 detectors have response outside that displayed in the figure, resulting in a 99.995 % operability. The standard deviation to mean ratio is $\sigma/\mu = 1.58$ %.

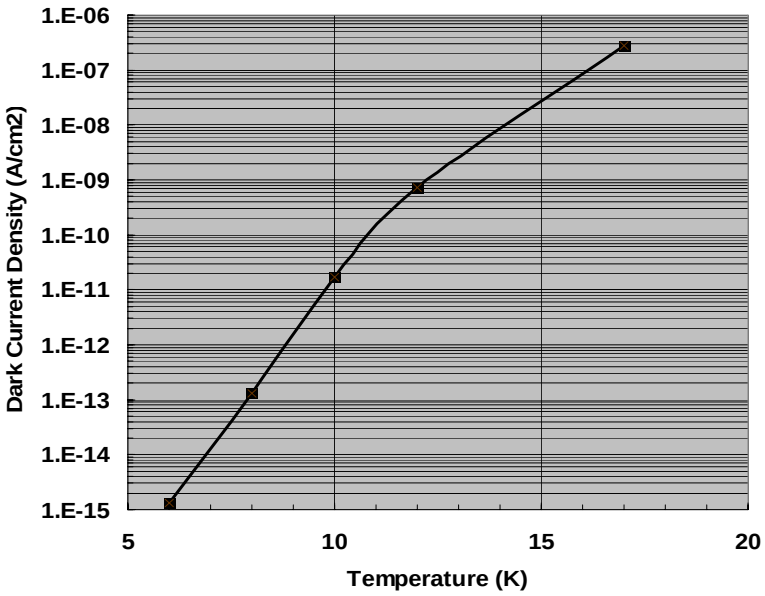


Figure 5. Dark current density versus temperature for a BIB detector optimized for low background applications

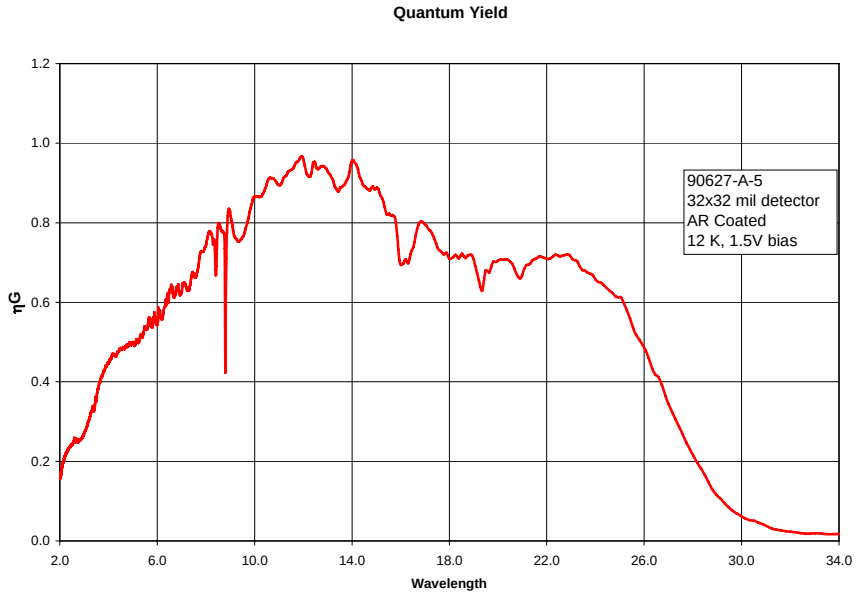


Figure 6. Quantum yield of an AR-coated Si:As BIB detector

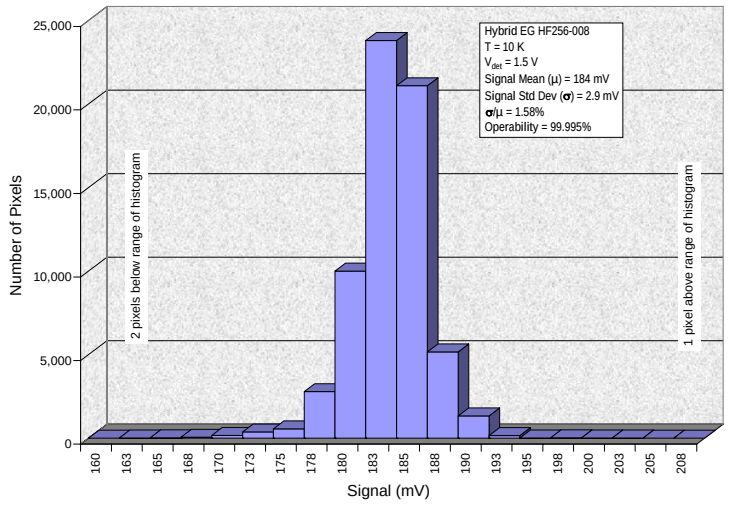


Figure 7. Detector response data for a 256 x 256 Si:As BIB Focal Plane Array

## 7. RECENT ROIC and BIB DESIGNS

Recent focus has been on designing larger format (1024 x 1024) read out integrated circuits and detector arrays. The ROICs (characteristics listed in Table I) and detectors designed have targeted both low and high background applications. Both types are in different stages of fabrication and are to be completed shortly. Testing of the 1024 x 1024 arrays will be completed immediately following fabrication. The ROICs are designed to interface with BIB detectors operating at ~ 10 K and also with Si p-i-n diodes operating at room temperature or colder if desired.

Table I. 1024 x 1024 ROIC Characteristics

| Parameter | Units | Value | Value |
|---|---|---|---|
| | | High Background | Low Background |
| Format | | 1024 x 1024 | 1024 x 1024 |
| Integration Mode | | Ripple | Ripple |
| Pixel Pitch | μm | 18 | 18 |
| Detector Material | | Si:As | Si:As |
| Band | μm | 5 - 28 | 5 - 28 |
| Integration Control | | Variable | |
| Read Noise | $e^-$ | < 1000 (10 ms τint) | < 40 |
| Dark Current | $e^-/s$<br>$e^-/s$ | < 12,800 @ 10 K<br>< 10 @ 6K | < 2 @ 6 K |
| QE | | > 57% | |
| Well Capacity | $e^-$ | ≤ 5.0 x $10^6$ Max<br>≥ 1.0 x $10^5$ Min | 1.0 x $10^5$ |
| Full Well Output Signal | V | 1.5 | 0.5 |
| Operability | % | > 99 | > 99 |
| Non-uniformity | % | < 2 | |
| Linearity | % | < 2 | < 5 |
| Frame Rate | Hz | < 100 | 1 (max) |
| Number of Outputs | | 16 | 4 |
| Data Rate | Pix/s/output | ≤ 7.0 x $10^6$ | 2.5 x $10^5$ (max) |
| Power Dissipation | mW @ max frame rate | < 115 | < 4 |

DRS' visible hybrid FPA technology is compatible with a multitude of legacy CMOS readout circuits including the 1024 x 1024 format described in Table I. This *p-i-n* detector architecture has allowed us to leverage the large investment in design and fabrication associated with these large format and other ROIC designs. Legacy ROICs provide operational simplicity for these visible arrays by using standard CMOS supply voltages resulting in low system power, weight and cost. The low noise/low power 1024 format selectable gain ROIC in Table I has selectable gain, windowing capability, integration time control and 16 outputs. The full array can be read out at frame rates as high as 100 Hz. Windowing allows a 256 x 256 sub-array that can be read out at 1,200 Hz. The array is 2-side buttable to 2048 x 2048, yielding a 4 times increase in FOV. DRS is currently processing *p-i-n* detector arrays suitable for FPA fab using this ROIC.

The *p-i-n* detector technology in combination with CMOS ROICs developed for infrared technology applications is being developed as an alternative to charge coupled devices (CCDs). The *p-i-n* detector/CMOS ROIC FPA technology limits FPA susceptibility to degradation in a radiation environment typically encountered by satellite-based sensors. Radiation tolerance of these devices can be further improved by utilizing radiation-hard design features and radiation qualified CMOS foundries.

Other advantages over CCD are realized by virtue of the large commercial CMOS foundry base. Future array designs will benefit from the continuing CMOS design/processing innovations. Increased circuit density will result in ever "smarter" FPAs with on-chip ADCs and other signal processing capabilities. These advances will be used to bring the noise performance to the level currently achieved by CCD arrays. Figure 8 shows a wafer with both 1024 x 1024 and 256 x 256 staring arrays and multi-band linear array types that are currently being processed for a satellite-based earth sensing application.

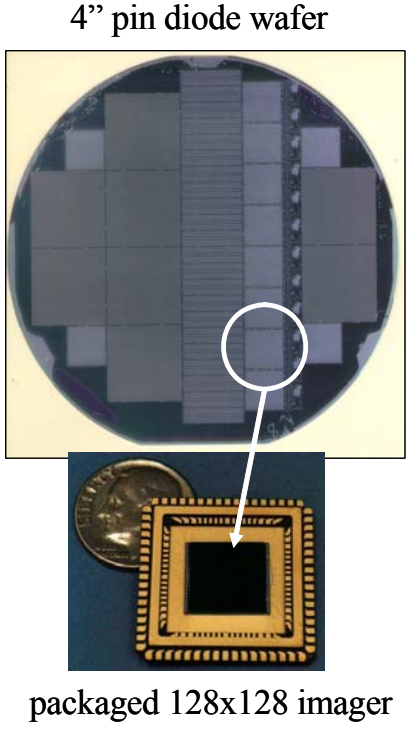


Figure 8. Wafer with both 1024 x 1024 and 256 x 256 staring arrays and multi-band linear arrays currently being processed for a satellite-based earth sensing application

## 8. POLARIZATION ARRAYS

Radiation emitted or reflected from a scene has three measurable properties: intensity, wavelength and polarization. Polarimetric imaging (PI) sensors measure both the intensity and polarization signatures of scene elements. Because

electromagnetic radiation is polarized after reflection from a specular surface, man made objects tend to have a polarization signature greater than natural background elements in a scene. Kirchoff's law dictates that thermal emission will also be polarized. Hence these polarization signatures span a broad wavelength spectrum including the visible through LWIR bands.

Polarimetric imaging can provide increased contrast between man-made objects and natural backgrounds. This ability can be used for target detection applications by highlighting man made objects in the scene. By imaging three or more separate polarization bands, image processing algorithms can extract a complete description of the linear polarization state of scene elements. This information can be used to estimate the surface normal orientation projected on the image plane. Algorithms have been devised which use this information for contrast enhancement in the LWIR band resulting in thermal images that have increased depth appearance analogous to a visible image of the same scene. This LWIR-specific technique also provides contrast for scene elements despite low thermal contrast typical seen at thermal crossover.

The utility of PI for targeting applications has been demonstrated in the visible waveband. False alarm rates are reduced significantly. Performance of these prototype visible polarimetric imaging devices has been constrained by several factors including their non-monolithic architecture. By applying the processing and imaging capabilities that we have developed and demonstrated on both Si:As BIB and HgCdTe arrays to the visible p-i-n diode arrays DRS can significantly improve the performance of prototype visible PI sensors based on commercial CCD arrays. DRS can apply the process techniques already demonstrated with LWIR FPAs to Si p-i-n arrays under development, enabling high performance visible wavelength polarimetric staring arrays suitable for potential SSA needs. One could imagine a sensor that used PI to discriminate man made objects such as satellites from natural objects such as stars.

Laboratory based polarimetric imaging sensors often utilize a rotating quarter wave plate, in conjunction with a single orientation wire grid analyzer. This PI configuration does not support real time imaging. To date, real time PI sensors have utilized division of aperture (multiple images of the same scene on a single array) or division of amplitude (beam splitters with multiple arrays) to realize real-time PI. These architectures offer real time imaging at the expense of sensor complexity. DRS pioneered a micropolarizer sensor architecture that eliminates the complex optical elements and alignment requirements while maintaining the real time PI capability.

The ability to monolithically pattern optical elements on the backside of thinned silicon detector wafers has been developed to fabricate large-format Si:As BIB arrays with integrated wire-grid micropolarizer arrays on the photon-incident side. This novel micropolarizer detector technology allows real time PI with an FPA that is easily integrated into sensors. Figure 9 shows a fully processed 5" wafer with a multitude of arrays and formats (128x128, 256x256) that include these monolithic wire grid elements in both stripe and checkerboard patterns. Some of the arrays have wire grid polarizers in stripe formats suitable for a push-broom sensor while others have a 2x2 checkerboard pattern such as shown in Figure 9.

Images from these arrays are processed to calculate three of the four Stokes parameters (S0, S1, S2) which completely describe the linear polarization state and are used in image processing algorithms for targeting applications and/or image enhancement. Figure 10 shows histograms of Noise Equivalent S1 and S2 from a PI sensor built from HDVIP LWIR HgCdTe FPA technology. Noise equivalent values below 5 μflicks are generally sufficient to produce polarization-enhanced images with minimal artifacts.

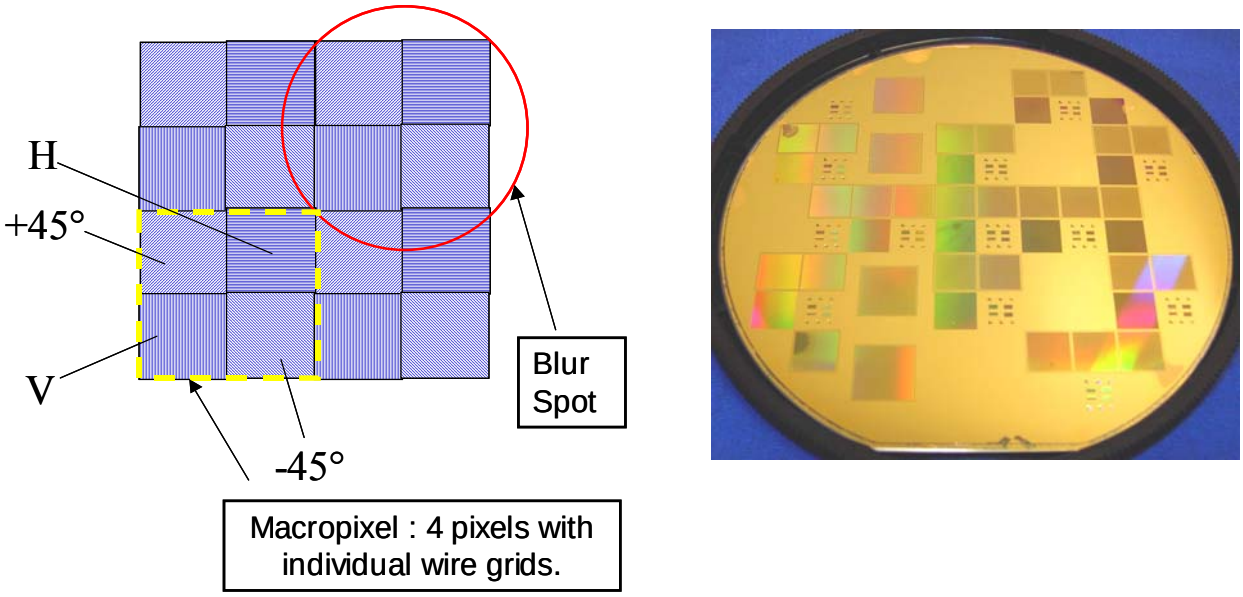


Figure 9. Checkerboard pattern of wire grid polarizers and photo of a fully processed 5" wafer with multiple array formats which include monolithic wire grid elements in both stripe and checkerboard patterns

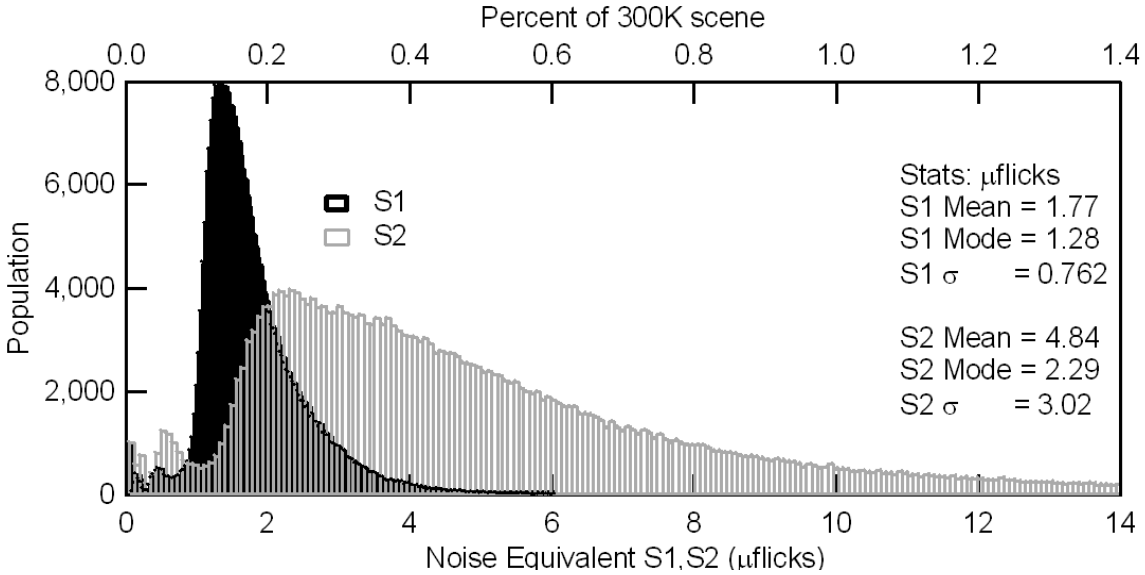


Figure 10. Noise Equivalent S1 and S2 histograms from an HDVIP LWIR HgCdTe FPA PI sensor

## 9. CONCLUSIONS

DRS manufactures HgCdTe and silicon detectors and FPAs in a variety of formats, from linear to 2-D arrays. HgCdTe HDVIP FPAs have been measured under a variety of flux conditions and at several operating temperatures. Silicon detectors covering the spectral range from visible to the very-long-wavelength infrared (VLWIR) have been fabricated and been optimized for low, moderate, and high infrared backgrounds. 1024 x 1024 BIB detector arrays and ROICs are in fabrication.

HDVIP HgCdTe 2.5 μm, 5.3 μm and 10.5 μm cutoff detectors have been fabricated into 320 x 6 linear arrays The MWIR detector array has a mean quantum efficiency of 89.2 % with a standard deviation to mean ratio, σ/μ = 1.51

%. NEI $\sigma/\mu$ = 3.0 % was measured with 100 % operability when running the array in the best detector select mode. 256 x256 Arsenic-doped silicon (Si:As) BIB detector arrays with photon response out to about 28 μm have been measured with a 99.995 % operability and a response standard deviation to mean ratio of 1.58 %. DRS has developed techniques that allow precision photolithographic backside processing on thinned silicon detector wafers enabling manufacture of monolithic high performance optical elements such as wire grid polarizers and diffractive lenslets on Si:As BIB arrays. This technique has been used to manufacture and demonstrate advanced sensors including real-time polarimetric imaging arrays capable of fully characterizing the linear polarization state of scene elements. Non-monolithic prototypes for the visible and LWIR wavebands have been assembled using commercial CCD imaging chips and LWIR HgCdTe arrays. DRS can apply the process techniques already demonstrated with LWIR FPAs to Si P-I-N arrays being developed and enable high performance visible wavelength polarimetric staring arrays suitable for potential SSA needs.

## 10. ACKNOWLEDGEMENTS

Thanks are due to our ITT and DRS colleagues, who contributed to the success of the technology demonstrations discussed in this paper.

## 11. REFERENCES

[1]. H.D. Shih, M.A. Kinch, F. Aqariden, P.K. Liao, H.F. Schaake, Appl. Phys. Lett. Vol. 83, 4157(2003).
[2]. M.A. Kinch, Proc. SPIE meeting, Vol. 4369, pp. 566-578 (Orlando, April 2001).
[3]. A.I. D'Souza, M.G. Stapelbroek, L. Dawson, P. Ely, C. Yoneyama, J. Reekstin, H-D Shih, M. Skokan, T. Teherani, J. Robinson, SPIE Vol. 5978. Paper 5978-18 of "Sensors, Systems, and Next-Gen. Sat. IX".
[4]. A.I. D'Souza, M.G. Stapelbroek, L. Dawson, P. Ely, C. Yoneyama, J. Reekstin, H-D Shih, M. Kinch, M. Skokan, T. Teherani, J. Robinson,, "SWIR to LWIR HDVIP HgCdTe Detector Array Performance", SPIE Proceedings, Vol. 6206, No. 62062H.
[5]. M.D. Petroff and M.G. Stapelbroek, *Proc. of the Meeting of the Specialty Group on Infrared Detectors* (IRIA-IRIS, Boulder, CO., 1985).
[6]. M.D. Petroff and M.G. Stapelbroek, U. S. Patent No. 4,568,960 (4 February 1986).
[7]. P. Galdemard, F. Garnie, P. Mulet, D. Reynolds, SPIE Proceedings, Vol. 4841, pp. 129-140, Instrument Design and Performance for Optical/Infrared Ground-based Telescopes; Masanori Iye, Alan F. Moorwood, Editors. March 2003.